

AttributionScanner: A Visual Analytics System for Model Validation with Metadata-Free Slice Finding

Xiwei Xuan^{1,†}, Jorge Piazentin Ono², Liang Gou^{2,†}, Kwan-Liu Ma¹, and Liu Ren²

Abstract—Data slice finding is an emerging technique for validating machine learning (ML) models by identifying and analyzing subgroups in a dataset that exhibit poor performance, often characterized by distinct feature sets or descriptive metadata. However, in the context of validating vision models involving unstructured image data, this approach faces significant challenges, including the laborious and costly requirement for additional metadata and the complex task of interpreting the root causes of underperformance. To address these challenges, we introduce *AttributionScanner*, an innovative human-in-the-loop Visual Analytics (VA) system, designed for metadata-free data slice finding. Our system identifies interpretable data slices that involve common model behaviors and visualizes these patterns through an *Attribution Mosaic* design. Our interactive interface provides straightforward guidance for users to detect, interpret, and annotate predominant model issues, such as spurious correlations (model biases) and mislabeled data, with minimal effort. Additionally, it employs a cutting-edge model regularization technique to mitigate the detected issues and enhance the model’s performance. The efficacy of *AttributionScanner* is demonstrated through use cases involving two benchmark datasets, with qualitative and quantitative evaluations showcasing its substantial effectiveness in vision model validation, ultimately leading to more reliable and accurate models.

Index Terms—Model validation, visual analytics, data slicing, data-centric AI, human-assisted AI.

I. INTRODUCTION

As machine learning (ML) technologies continue to prevail in various domains, the importance of model interpretation and validation has grown significantly. Identifying a model’s failure and understanding the underlying reasons are crucial in promoting greater model accuracy, transparency, and accountability. A powerful technique supporting this effort is data slice finding [1], aiming to identify problematic data subgroups, referred to as slices, which often arise from under-represented samples or biased datasets [2]. These data slices are commonly defined by descriptive metadata, with contextual details of the model’s input such as feature descriptions, data collection details, and other relevant information.

After problematic data slices are identified, the remedial strategies often involve model training or fine-tuning with these slices to bolster the model’s overall reliability [3]. To enhance the trustworthiness, eXplainable Artificial Intelligence (XAI) [4] are also utilized in recent techniques to reveal potential causal factors adversely impacting the model and apply targeted model regularization [5] to improve the performance.

Despite the promising benefits of these techniques, several hurdles remain unaddressed for a thorough model validation.

Challenges of Data Slice Finding. State-of-the-art methods for data slice finding demand extensive metadata associated with each instance. Many works use pre-existing metadata collected together with the dataset [6]–[8], and others apply pre-trained vision-language models to generate descriptive data [3]. However, there are challenges hindering their applications—On the one hand, it requires significant effort to collect descriptive metadata. On the other hand, trained with general-purpose data, vision-language models can generate erroneous results in domain-specific scenarios. In situations where neither metadata nor suitable pre-trained models are available, obtaining interpretable data slices becomes challenging: requires manual examination of numerous instances or computationally expensive model training [9], [10].

Challenges of XAI for Vision Models. If troublesome data slices have been identified, it also requires non-trivial efforts to uncover the root causes of a model’s failure. Even with the advanced human-friendly XAI techniques, there still exist a few challenges. Predominantly, most model explanation methods are instance-based, conducting a thorough examination of all instances to derive conclusions based on a big picture is practically unfeasible [11]–[14]. Moreover, the insights we can obtain from existing methods are often not actionable, which means what the common failure patterns are and how to address them remain vague and demands further study.

Our approach. We present *AttributionScanner*, a Visual Analytics (VA) system designed to address the above challenges, providing an interpretable vision model validation framework with metadata-free slice finding. Our innovative workflow employs attribution-based explanation techniques to create interpretable feature representations for slice finding, sorting through unstructured image data into slices with common model behaviors. Moreover, we explain the discriminating features of each data slice via visual summaries, called *Attribution Mosaic*, to guide users in explaining model’s behaviors and detecting potential issues, thus facilitating model validation. Additionally, *AttributionScanner* integrates a human-in-the-loop approach to rank and annotate the problematic data slices based on common error types such as mislabeled samples and spurious correlations. Our approach enables users to apply these annotated slices to enhance the model, by correcting the identified errors on either the model or data side. Our main contributions include:

- *AttributionScanner*, a novel framework and VA system to validate vision models with data slice finding. Unlike existing

¹ Department of Computer Science, University of California, Davis, CA 95616, USA. E-mails: {xwxuan, klma}@ucdavis.edu.

² Bosch Center for Artificial Intelligence (BCAI), Bosch Research North America. E-mails: {jorge.piazentinono, liang.gou, liu.ren}@us.bosch.com.

[†] This work was done when the authors worked with BCAI.

methods, *AttributionScanner* removes the resource-intensive need for metadata to generate interpretable data slices.

- A design for slice summarization, *Attribution Mosaic*, illustrating the significant pattern of model behaviors in data slices, which reduces the effort in conventional approaches of examining a large volume of individual data samples.
- An iterative workflow supporting model validation and enhancement, which ensures generated insights are actionable, enabling users to swiftly detect, understand, and fix model issues related to spurious correlations and mislabeled data.
- Qualitative and quantitative evaluation. We underscore the efficacy of *AttributionScanner* through two use cases with qualitative and quantitative evaluation, highlighting its ability to identify and mitigate hidden model issues.

This paper is structured as follows: in Sec. II, we review related work on data slice finding and XAI that is relevant to our work. Sec. III outlines the methodology and system design of *AttributionScanner*. In Sec. IV, we illustrate two use cases showcasing how *AttributionScanner* can be utilized for vision model validation. An evaluation of our system and experts’ feedback are discussed in Sec. V. Lastly, we present our future work and conclusions in Sec. VII.

II. RELATED WORK

Our method, *AttributionScanner*, leverages insights from both Data Slice Finding and XAI techniques to pinpoint problematic data slices in vision-based models. This provides a brief overview of the relevant literature on these two topics.

A. Data Slice Finding

Data slice finding technique is used to identify data subsets where ML models underperform. These subsets are usually defined by a combination of feature-value pairs extracted from tabular metadata. However, the exponential search space associated with this task makes it a challenging problem. To overcome this challenge, heuristics have been presented to approximate the solution. Barash et al. [15] introduced a Combinatorial Modeling-based approach that enumerates the space of value combinations in tabular data up to a set number of parameters. Similarly, Slice Finder [6] uses a decision tree heuristic to identify interpretable data slices that can be described by tree rules. Despite the advantages of heuristics, they may miss important data slices. Therefore, new techniques have been developed to enable the exhaustive search of data slices using novel formulations and parallel architectures. DivExplorer [1] employs frequent pattern mining to enumerate all candidate slices in the data and identify the most relevant ones based on frequency or metric divergence. In contrast, SliceLine [7] introduces a vectorized formulation for slice finding, which can be easily deployed in parallel devices.

The aforementioned methods necessitate structured metadata to segment datasets into meaningful subgroups, a requirement challenging to meet, especially in domains with large volumes of image or text data where detailed meta-information may be scarce. To address this, a prevalent approach involves encoding data samples into the model’s latent space, followed by clustering to group the data and pinpoint problematic

slices. For instance, GEORGE [9] employs over-clustering alongside Group Distributionally Robust Optimization [16] to automatically detect and rectify distribution shift-induced errors. Spotlight [10] adopts a soft-clustering strategy, evaluating performance metrics per cluster and pinpointing clusters with the highest performance drops as data slices for user review. Similarly, UDIS [17] implements hierarchical clustering and further GradCAM [12] visual explanations for data slice examination. VisCUIT [18] allows a deeper exploration of the UDIS data slices by enabling slice comparison and the exploration of neuron activations per slice. Although these methods can support the identification of problematic slices, users have to delve into individual samples to understand model failure reasons. Domino [3] mitigates this by utilizing a pre-trained vision-language model for generating textual descriptions of slices, encoding images into model embedding, and clustering them based on shared visual attributes. However, this method’s reliance on pre-trained models for slice identification and explanation can backfire if there’s a significant domain mismatch between the dataset being evaluated and the pre-trained model, possibly yielding unmeaningful slices. In Sec. III, we introduce a methodology capable of producing explainable slices independently of such pre-trained models.

Visualization has also proven effective in identifying problematic subgroups of data. Kahng et al. introduced a data cube analysis method [19], in which the performance of models was assessed on data slices defined by all pairwise combinations of data features. Meanwhile, FairVis [20] enables users to manually slice and inspect data slices based on domain knowledge to identify potential model biases. Similarly, Errudite [21] came up with a domain-specific language to allow the data slicing of textual documents based on linguistic features and model testing under specific conditions. Although manually slicing the data is useful for model analysis, this approach is not scalable since there could be an exponential number of slices to evaluate. To address this issue, SliceTeller [2] combined an automatic slice finding algorithm with a visual analytics tool to allow the analysis and iterative refinement of models. However, it still required structured metadata in order to produce meaningful data slices. In Sec. III, we present a visual analytics tool that requires no metadata or prior information to produce meaningful data slices.

B. XAI Techniques for Neural Networks

Given the widespread adoption of deep learning models, there is significant interest in understanding their prediction processes. In particular, visualization-based XAI methods have gained popularity due to their ability to produce intuitive and meaningful results and be applied to explain various deep Convolutional Neural Networks (CNNs). One genre is localization-based explanations, namely attribution heatmaps, which highlight image regions mostly contributing to a specified class prediction, providing class-discriminative localization to support model interpretation. Class Activation Maps (CAM) [11] is a pioneering method, but it requires a specific network architecture, namely the global average pooling layer, to generate visualizations. GradCAM [12] addresses this limitation by using gradients to compute model attributions. In our

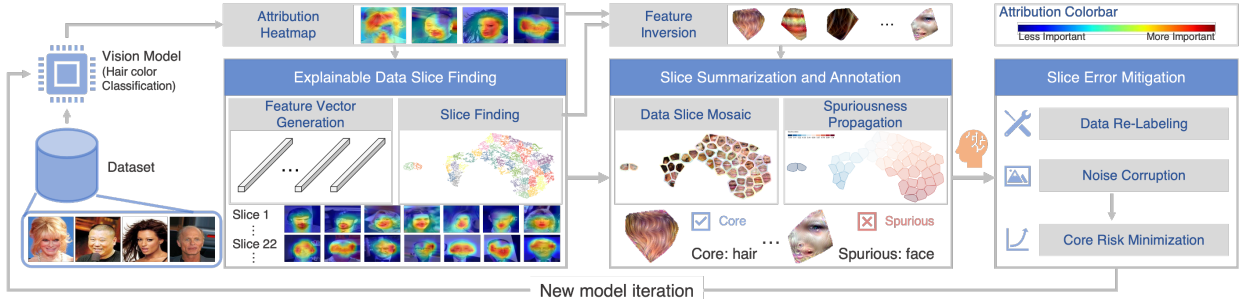


Fig. 1: *AttributionScanner* workflow involves three phases: *Explainable Data Slice Finding*, *Slice Summarization and Annotation*, and *Slice Error Mitigation*. The first phase: GradCAM is used to assist the generation of feature vectors and then obtain data slices. The second phase: users can identify and annotate slice error types such as core/spurious correlations and noisy labels with the help of *Attribution Mosaic* and *Spuriousness propagation*. The third phase: the annotation and user-verified *Spuriousness* are used on the ML side to mitigate slice errors, including (1) *Data re-labeling* if considered necessary, and (2) *noise corruption* and *Core Risk Minimization (CoRM)* applied if spurious correlations are detected.

work, we utilize GradCAM attribution heatmaps in two ways: firstly, we use them to explain model predictions on single images. Secondly, we interpolate the attributions into weight matrices at the latent space to obtain attribution-weighted feature vectors, which are used to obtain and visualize data slices with similar model attribution patterns.

Another popular approach for understanding model behavior is optimization-based visual explanations. Feature Visualization [13], [22] creates images that maximally activate specific neurons, channels, or layers of a neural network, which focuses on understanding features that a model is sensitive to. Feature inversion [23] seeks to understand the information encapsulated in a group of spatial feature vectors. Specifically, it visually elucidates the shared patterns significant in those latent vectors from the model’s perspective.

III. *AttributionScanner*

In this section, we introduce *AttributionScanner*, a novel approach for interpretable ML model validation with metadata-free, data slice-level analysis. To foster a thorough understanding of our system, we first outline the requirements that shaped our design choices. Then, we delve into the visual components of *AttributionScanner* that enable interpretable model validation. We then detail our slice computation and summarization method, which allow us to generate data slices with consistent model attribution without additional metadata. Finally, we show how we leverage the insights obtained from our system to enhance the model.

A. Design Requirements

Slice finding has garnered increased attention due to its potential to facilitate a thorough ML model evaluation. However, this task is particularly challenging in the realm of vision models considering the inherent unstructured nature of vision data. A pivotal shortcoming we observed in existing approaches is their dependency on metadata, including pre-collected or vision-language model-generated ones, to compute meaningful data slices. However, the acquisition of metadata is resource-intensive, demanding substantial human effort and financial investment. Additionally, the vision-language

models are commonly trained on general-purpose datasets, potentially leading to inaccurate or biased results in specific domains. Stemming from these observations, we delineated the subsequent requirements for a system capable of conducting metadata-free, slice-driven model validation:

- R1. Metadata-free.** Our method should yield meaningful data slices without metadata, i.e., descriptive information other than the model’s training data.
- R2. Interpretability.** We should provide sufficient and intuitive information to enhance model transparency. Diverging from prior metadata-free approaches that lack explanation capability, our system should enable both intuitive explanations of a data slice’s shared attributes and inspection of individual instances for insight verification as needed.
- R3. Slice Overview.** Mandatory manual inspection of individual images is impractical for model validation, especially with a high volume of data. To enhance efficiency, our system should provide a visual summary of data slices, depicting each data slice’s key features and attributions.
- R4. Actionable insights.** The system should ensure the obtained insights are actionable, which requires careful design of visual guidance, issue annotation, and corresponding model regularization. The framework should allow for further expert engagement, such as re-labeling or model re-training, to enhance model performance.

B. System Workflow

AttributionScanner is a human-in-the-loop system, taking as input an image dataset and a trained CNN for image classification, and yielding interpretable data slices to assist human experts in metadata-free vision model validation.

A workflow of our approach is presented in Fig. 1, where we foster explainable slice finding without metadata (**R1**, **R2**) by leveraging XAI technique GradCAM [12] and Feature Inversion [13]. The first “explainable data slice finding” phase interpolates model attributions from GradCAM into the latent space to craft attribution-weighted feature vectors, which enable us to form an attribution representation space with locally consistent model attributes (**R1**). Then we conduct clustering over this space to generate data slices. Although the produced slices maintain consistent attributions, they still

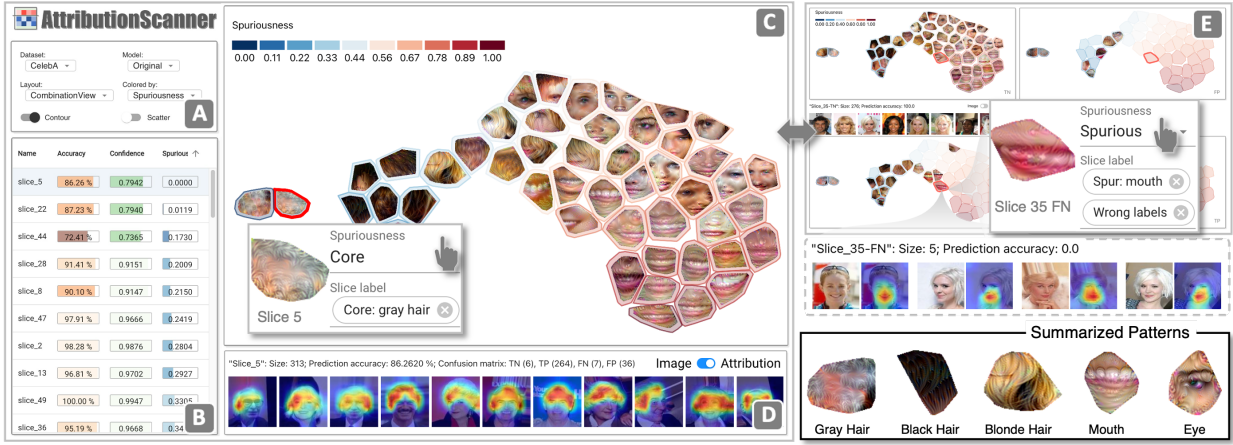


Fig. 2: *AttributionScanner* applied to the model validation of a hair color classifier trained on the CelebA dataset. **A** System Menu, enabling the selection of dataset, model, and visualization options (Layout, Confusion Matrix, Scatter Plot/*Attribution Mosaic*, and Contour Visibility). **B** Slice Table, showing slice metrics. **C** *Attribution Mosaic*, showing a visual overview of all data slices, which can also be displayed as a confusion matrix view (**E**). **D** Slice Detail View, showing individual images or Attribution Heatmaps belonging to a selected data slice.

demand significant human effort to identify and understand their shared patterns. To streamline slice exploration and issue detection, the “slice summarization and annotation” phase introduces *Attribution Mosaic*, which visually elucidates each slice’s dominant attributions (**R3**), synchronized with instance-level heatmaps for insight verification (**R2**). Upon user annotation of an issue like “spurious correlations”, our Spuriousness Propagation method automatically estimates a spuriousness score for each slice to help users uncover other hidden model biases (**R4**). Afterward, our workflow enables the mitigation of detected issues in data or model, corresponding to the “slice error mitigation” phase (**R4**).

The rest of this section delineates our interface for data slicing-based model validation, explains our presented data slicing and summarization approach, discusses design considerations, and demonstrates how the model can be fine-tuned to rectify detected slice issues.

C. System Interface

AttributionScanner is comprised of four main components. Fig. 2 depicts a use case where our system is used to validate a hair color classification model.

The System Menu (Fig. 2 **A**) provides options for dataset and model selection, visualization layout configuration, and color encoding choice. Two visualization layouts are available: Combination view and Confusion Matrix view, allowing for an overall view of data slices or a more detailed inspection categorized by error types (**R3**). The provided color encoding choices include Slice Name, Slice Accuracy, Slice Confidence, and Spuriousness Probability, adaptable to user requirements.

The Slice Table (Fig. 2 **B**) presents various slice performance metrics to facilitate dataset navigation. Available metrics include Accuracy, Confidence, and Spuriousness Probability, which is produced by the Spuriousness Propagation method upon user annotation (Sec. III-E). This table assists in detecting intriguing patterns, like high accuracy with wrong attributions possibly indicative of model biases. On the other

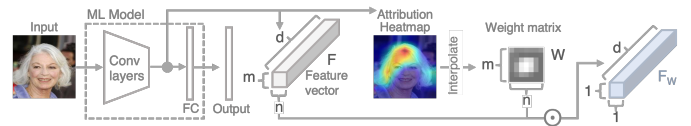


Fig. 3: Attribution-weighted feature vector generation. An image is forwarded through CNN, where the corresponding feature vector F and attributions heatmap A can be extracted. Through linear interpolation of A to the latent space, we obtain the weight matrix W to calculate the attribution-weighted feature vector F_w .

hand, low accuracy with correct attributions indicates the potential existence of mislabeled data (**R3**, **R4**).

Our system’s third component is the *Attribution Mosaic*, rendering the dominant visual patterns of each slice with respect to the model’s decision (**R2**, **R3**), either in a unified form (Fig. 2 **C**) or segregated by the model’s confusion matrix (Fig. 2 **E**). The design method for this view is detailed in Sec. III-E. Moreover, *Attribution Mosaic* incorporates visualization of user-specified metrics through the coloration of mosaic boundaries, providing a vital guide in pinpointing problematic slices (**R3**). Annotation of a slice is facilitated by a double-click action on a mosaic tile, allowing for effortless insight collection (**R4**).

The Slice Detail View (Fig. 2 **D**) showcases individual image samples of the selected data slice, rendering either images or attribution heatmaps. This view enables an in-depth examination of each slice (**R2**).

D. Explainable Data Slice Finding

In this section, we delineate our Explainable Data Slicing method. Our approach presumes a typical CNN model architecture, comprising a sequence of convolutional layers succeeded by a fully connected (FC) layer, a commonality across most CNN models [12], [24], [25].

The process unfolds in three phases: initially, we create attribution-weighted feature vectors utilizing the interpolated attribution masks in the latent space. Subsequently, we derive

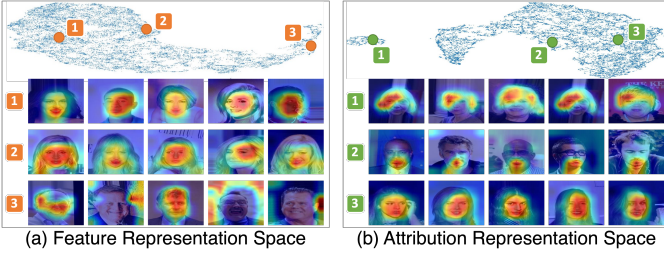


Fig. 4: Comparison of the representation spaces for the hair color classification model. (a) Feature representation space computed on original feature vectors. (b) Attribution representation space computed on attribution-weighted feature vectors.

an attribution representation space that maintains neighbor consistency in terms of model attributions and compute data slices. Lastly, we employ the Feature Inversion [23] to distill shared visual patterns per slice and visualize these patterns alongside model performance indicators in *Attribution Mosaic*.

(1) Attribution-Weighted Feature Vector Generation

In this section, we illustrate the process of generating attribution-weighted feature vectors based on attribution heatmaps (R1, R2). It is notable that *AttributionScanner* accommodates interchangeable attribution explanation techniques, such as CAM [11], GradCAM [12], or RISE [14] (R2). Our prototype leverages GradCAM due to its demonstrated efficacy via sanity checks [26] and its prevalent usage for model validation in the ML community [5], [17], [27]–[31].

As shown in Fig. 3, an input image is processed by the model to extract the feature vector F , and a back-propagation is conducted from the model’s predictions to obtain the GradCAM attribution masks. While a conventional approach is to depict the mask as a heatmap for the instance-level explanation, we augment its explanation capability to the latent space to foster a more comprehensive understanding of the model’s attribution patterns. Specifically, we apply linear interpolation to map image-sized masks into the latent space, yielding a weight matrix $W \in \mathbb{R}^{m \times n}$. Then the normalized W with $\sum_{i=1}^m \sum_{j=1}^n W_{ij} = 1$ is used to compute the weighted average of F . The resulting attribution-weighted feature vector $F_W \in \mathbb{R}^{1 \times 1 \times d}$ can be mathematically expressed as:

$$F_W = F \odot W = \sum_{i=1}^m \sum_{j=1}^n F_{ij} W_{ij}. \quad (1)$$

(2) Data Slice Identification

To derive meaningful data slices exhibiting similar attribution patterns (R1, R2), we construct an attribution representation space using the attribution-weighted feature vectors. Fig. 4 provides a qualitative comparison of the **feature representation space** (derived from the original feature vectors) and the **attribution representation space** (derived from the attribution-weighted feature vectors). For both spaces, we utilize UMAP [32] for dimensionality reduction to the 2D space. At each representation space, three points are randomly sampled and their nearest neighbors are obtained to examine the consistency of their corresponding attribution heatmaps. As showcased in Fig. 4, it is obvious that the neighbor instances’ model attributions from the original space are not

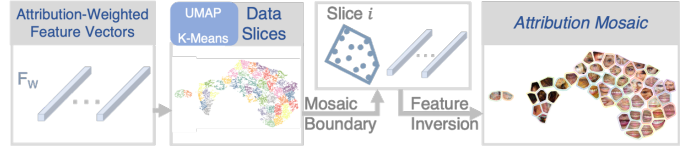


Fig. 5: *Attribution Mosaic* generation. After acquiring attribution-weighted feature vectors (F_W), we compute data slices within the attribution representation space. Then Feature Inversion is conducted according to F_W and the mosaic boundary of each slice to visualize their common patterns, forming *Attribution Mosaic*.

similar, while our constructed attribution representation space has greater local consistency concerning model attributions. Therefore, our attribution representation space provides a solid basis for computing interpretable data slices with coherent attribution patterns (R2).

On top of our constructed attribution representation space, we proceed by clustering the samples with K-Means to obtain data slices. Similarly to DOMINO [3], we apply over-clustering by incrementing the number of clusters and monitoring the model attribution consistency within each slice, until a coherent grouping of samples is attained. This measure helps prevent the omission or overlooking of rare slices, ensuring a comprehensive slice identification.

E. Slice Summarization and Annotation

(1) Attribution Mosaic

Although we have generated slices with consistent model attributions, validating the attribution correctness of each slice necessitates individual inspection of their encompassed data samples. This process is labor-intensive and time-consuming, posing the risk of overlooking or misidentifying critical issues. Therefore, a more efficient method to encapsulate the essence of each data slice is imperative. In response, we introduce *Attribution Mosaic*, a novel visualization technique that elevates Feature Inversion to visually summarize data slices in a mosaic depiction (R3). We present the pipeline in Fig. 5. First, after the execution of data slice finding (Sec. III-D), we compute the convex hull of each slice based on the projected points in the 2D space. We then distill each slice’s predominant visual patterns via Feature Inversion, integrating the shape constraint of the convex hull. The final landscape featuring slices’ attribution summaries is presented as *Attribution Mosaic*.

Slice Summary. A pivotal step in generating *Attribution Mosaic* involves visually summarizing the significant pattern in each slice (R3). As discussed in Sec. II-B, Feature Inversion visualizes common patterns across a group of feature vectors [33]–[35]. We utilize this technique on the attribution-weighted feature vectors of each slice to visualize their shared attributions. Additionally, we enhance the quality of synthesized images by initializing them with the average of the original images instead of Gaussian noises [34] and parameterizing them in the Fourier space [35], making them better aligned with natural images rather than less-interpretable artificial patterns. The optimization process is defined by:

$$x^* = \arg \max_{x \in \mathbb{R}^{W \times H \times C}} (\ell(\phi(x), \phi_0) + \lambda R(x)), \quad (2)$$

where $\phi : \mathbb{R}^{W \times H \times C} \rightarrow \mathbb{R}^d$ is the representation function; ϕ_0 is a target feature activation; $\ell(\ast)$ is the loss function where the Euclidean Loss is used here, and $R(x)$ is a Total Variation (TV) regularization term to improve the quality of results [23]. In our scenario, we designate the optimization target, ϕ_0 , to be the average of attribution-weighted feature vectors of a data slice, and assign the representation function to the model’s convolutional modules. We obtain an image x^* to minimize the loss function, thereby visualizing the shared attribution patterns within a data slice from the model’s perspective.

Mosaic Boundary Generation. The main purpose of this stage is to devise a clear layout enabling effortless exploration of diverse attribution patterns across slices. Merely obtaining and displaying the Feature Inversion results over the projected cluster centroids leads to overlapped visualizations, hindering effective user exploration. We design a mosaic layout, optimized for space-efficiency in information representation. Specifically, we compute convex hull [36] of each slice in the attribution representation space, yielding a convex hull for every slice with no overlap amongst them.

Mosaic drawing. Given that the convolutional modules take rectangular-shaped input, the original Feature Inversion algorithm solely generates rectangular visualizations. To preserve equivalent visualization in a mosaic form, we use our generated mosaic boundary as a constraint for optimization. Namely, we define the shape of x^* as the minimal rectangle encompassing the corresponding convex hull, and in each iteration, we zero out pixels outside the hull, compelling the optimization to concentrate on the interior pixels. After rendering all feature visualizations, they are exhibited at their respective positions within the *Attribution Mosaic*.

(2) Slice Annotation and Spuriousness Propagation

The *Attribution Mosaic* facilitates rapid comprehension of the main content of different slices, supporting the identification of potential errors in data or models (R4). A prevalent and harmful issue in ML models, highly visible through *Attribution Mosaic*, is “spurious correlation”, where a model erroneously utilizes irrelevant image features for classification. For instance, in hair color classification, a model should make decisions according to hair features, termed as “correct/core correlation”, while the use of other features (e.g., background or facial attributes) denotes “spurious correlation.”

Such spurious correlations, regardless of model accuracy, pose substantial challenges including poor generalization in production [37] and AI fairness issues [38]. We introduce a metric termed Spuriousness probabilities to streamline the detection of spuriousness, ranging from 0 to 1, indicative of the likelihood of spurious correlation existence. We employ the Label Spreading method [39] to propagate user annotated spurious/core information to other slices. Specifically, the minimal input requirement from users is one slice annotation of “core” (Spuriousness=0) or “spurious” (Spuriousness=1), and then *AttributionScanner* will propagate this information to create a Spuriousness Probability for the rest slices.

The Spuriousness probabilities obtained through the *Attribution Mosaic* offer two benefits. First, they streamline slice exploration by highlighting potential spurious correlations,

TABLE I: System Design Considerations.

Design Components				System Capabilities			
Slice Table	Slice Detail View	Scatter Plot	Attribution Mosaic	Slice Performance	Slice Attribution	Instance Performance	Instance Attribution
✓	✓			✓			✓
✓	✓	✓		✓		✓	✓
✓	✓		✓	✓	✓	✓	✓

supporting identifying and assessing problematic slices. Second, after users’ verification, these probabilities inform the model-side strategies for issue mitigation (Sec. III-G) (R4).

F. System Design Considerations

In designing *AttributionScanner*, various configurations of visual components’ combinations have been evaluated to ensure optimal system capabilities to fulfill our design requirements discussed in Sec. III-A, as outlined in Table I. Our system should be capable of providing four-faced information: (1) slice performance indicator (R3), (2) slice attribution overview (R2, R3), (3) instance performance indicator (R2), and (4) instance attribution inspection (R2, R4). The notions in “design components” are consistent with Fig. 2.

In Table I, the initial configuration, “Slice Table & Slice Detail View,” is capable of presenting slice performance indicators and instance attributions. However, the numerical matrices of performance indicators are not sufficient in guiding users to uncover hidden model issues, such as spurious correlations that can happen regardless of high or low performance. A subsequent iteration included a scatter plot showing the attribution representation space. This configuration enables the system’s instance performance indicator capability but still misses the slice attribution overview. To the best of our knowledge, there exist few approaches that visually elucidate potential model spuriousness in scale, where our third configuration fulfills this gap — “Slice Table & Slice Detail View & *Attribution Mosaic*,” which comprehensively satisfies all the essential system capabilities and fulfills our design requirements.

Attribution Mosaic, alongside the Slice Table and Slice Detail View, enriched the system’s ability to provide granular insight into both slice and instance-level attributions and performance indicators (R2, R3). The coordinated Slice Table and *Attribution Mosaic* can guide users to pinpoint hidden issues, and the Slice Detail View enables users to further verify their insights (R4). This robust configuration underscores our meticulous design process in assuring that *AttributionScanner* is not only capable of furnishing critical insights but also does so in an intuitive and user-friendly manner.

The tabulated design considerations and the ensuing choice of system component configuration aim at maximizing the system’s utility and user-centric functionality. With our finalized configuration (the last row of Table I), users are empowered with sufficient support for problem detection, interpretation, and mitigation in the model validation.

G. Slice Error Mitigation

One effective approach to mitigating spurious correlations in ML models is through model re-training, which can improve the model’s robustness without changing its architecture. We leverage the Core Risk Minimization (CoRM) method

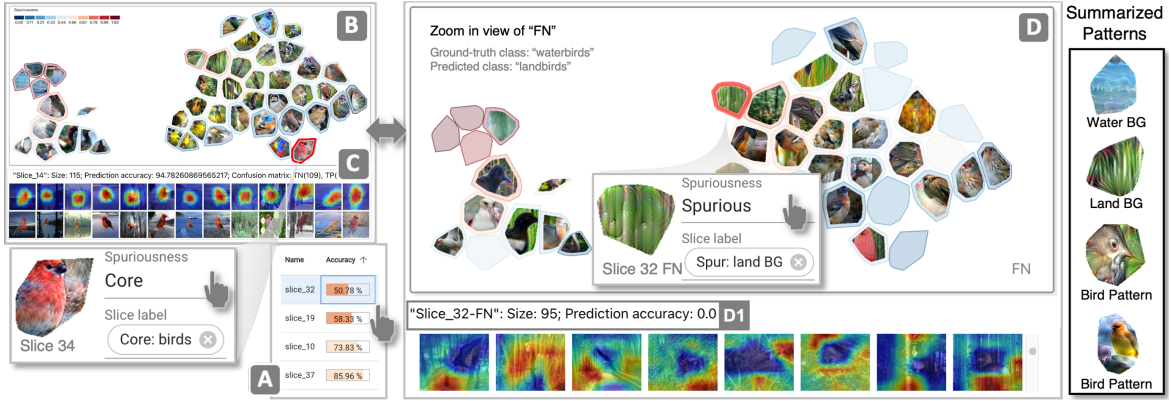


Fig. 6: *AttributionScanner* applied to the validation of a bird category classification model trained on the Waterbirds dataset. The user finds the correct model behavior (bird patterns) corresponding to a well-performed *Slice 34* and annotates it as “core: birds” **B** and **C**. By switching the *Attribution Mosaic* to the confusion matrix view **D** and investigating the underperformed slices with accuracy sorting **A**, the user identifies a problematic *Slice 32* that has high false negatives **D1**, which turns out to use spurious feature of land backgrounds (BG) to predict landbirds.

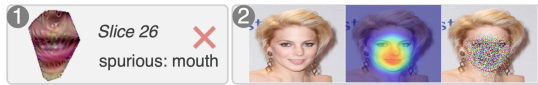


Fig. 7: Example of spurious correlation mitigation with CoRM for hair color classification: **1** The *Attribution Mosaic* indicates a problem with a spurious feature: mouth. **2** An example of how noise is occupied by CoRM: Original Image (left), GradCAM activations (middle), noise added to the spurious regions of the image (right).

introduced in [37]. CoRM corrupts non-core image regions with random Gaussian noise and retrain the model using the noise-corrupted data, which has been shown to be effective in mitigating a model’s reliance on spurious features.

We first export slices with high Spuriousness probabilities, indicating undesired correlations. For the images in these slices, the model attribution masks (e.g., GradCAM masks) highlight spurious regions and we utilize such masks to add random Gaussian noise to spurious regions. For a single image, this process can be represented by $\mathbf{x}' = \mathbf{x} + \mathbf{m} \odot \mathbf{z}$, where \mathbf{x} is the input image, \mathbf{m} is the attribution mask, and \mathbf{z} is the generated Gaussian noise matrix. All these three variables are of the same size as the input image, and \odot denotes the Hadamard product. Fig. 7 shows some examples of this operation, with exaggerated noise for presentation purposes. After replacing the original data with these noisy-corrupted slices, we retrain the model and evaluate whether spurious correlation has been reduced (**R4**). In Sec. V, we explain the evaluation metrics we use to quantify the effectiveness of *AttributionScanner* in mitigating spurious correlations.

IV. CASE STUDIES

In this section, we present two case studies with publicly available vision datasets to benchmark and evaluate the capabilities of *AttributionScanner*. The primary objective of these case studies is to demonstrate how *AttributionScanner* empowers ML experts and practitioners to detect, evaluate, and interpret potential issues in vision models. Fig. 8 illustrates common usage patterns of our system: users can begin the

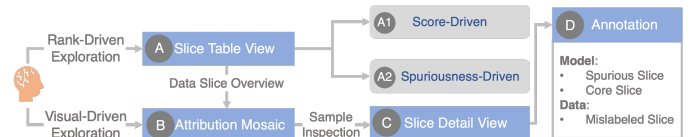


Fig. 8: Usage patterns for *AttributionScanner* derived from case studies. The analysis can start with **A** a rank-driven exploration (ranking the slices by **A1** score (e.g., model accuracy) or **A2** spuriousness), or **B** a visual-driven exploration. After inspecting slice summary in *Attribution Mosaic* (**B**), they can inspect individual samples in the Slice Detail View (**C**). Finally, they can annotate their insights (**D**).

analysis with either a rank-driven evaluation **A** or a visual-driven evaluation **B**. Once a slice of interest is identified, users can delve deeper into individual samples in the Slice Detail View **C**. Finally, the user can annotate the data slices and continue their analysis **D**.

A. Hair Color Classifier Validation - Finding Edge Cases

• **Overview.** This case study involves the Large-scale CelebFaces Attributes (CelebA) dataset [40] with 202,599 number of face images. The label of each image is one of $\{not\ gray\ hair, gray\ hair\}$, refer to labels $\{0, 1\}$, respectively. With the train, validation, and test splits of $(8 : 1 : 1)$, we adopt transfer learning to train a ResNet50 [25] binary image classifier. After iteratively fine-tuning hyper-parameters, we obtain a model with 98.03% classification accuracy. The ML experts would then explain and troubleshoot this hair color classifier with *AttributionScanner* based on these settings: $n_neighbors = 5$, $min_dist = 0.01$, and $n_components = 2$ for the UMAP algorithm, and $n_clusters = 50$ for K-Means.

• **Does the model behave correctly on well-performing slices?** One basic expected behavior for a hair color classification model is to catch hair features. At first glance of the *Attribution Mosaic* (Fig. 2 **C**), ML experts notice *slice_22* and *slice_5* on the left, which lie separately with others on the *Attribution Mosaic*. Their mosaic visualizations indicate gray hair patterns, which means the model uses the correct features, i.e., core features. By verifying the corresponding

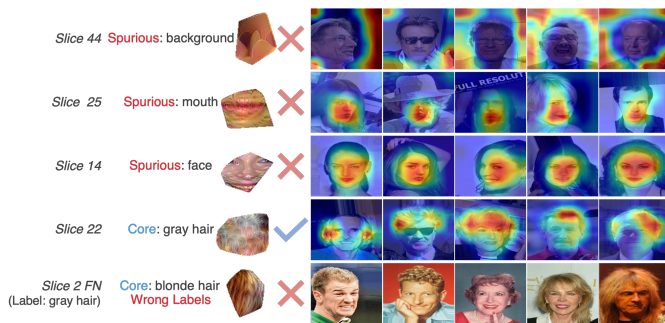


Fig. 9: Examples of findings when ML experts validate a hair color classifier, where experts discover slices corresponding to the model’s core/spurious correlations and wrong labels.

attribution heatmaps (Fig. 2 D), they confirm the correctness of this insight and annotate both slices as *core feature* with description *Core: gray hair*. Upon experts saving the annotation, *AttributionScanner* automatically propagates the annotation and provides a Spuriousness probability of each slice. With this guidance, the experts observe many slices lying on the right of *Attribution Mosaic* have higher Spuriousness probabilities (Fig. 2 C E). Their mosaic visualizations do not show any hair patterns, leading to valid doubts that the model does not behave correctly on such slices. Besides, they also notice that the model has correct predictions on these slices (with 100% prediction accuracy). This makes them worry that the model is largely biased by spurious features. Through investigation, they find the model mistakenly utilizes mouth and eyes to predict hair color for those top-performed slices, such as *slice_25*, *slice_14*, and *slice_2* (Fig. 9).

• **Why slices underperform?** The experts are also eager to investigate the underperformed slices. By sorting the Slice Table (Fig. 2 B) by ascending order of accuracy, they notice the model only achieves 72.41% accuracy on *slice_44* and find that the slice’s visualization only shows colorful patterns without any recognizable content. After checking the attribution heatmaps, they find that the model mistakenly uses image backgrounds to make hair color predictions (Fig. 9). This spurious correlation issue stands out, and they annotate this slice as “spurious” with the description “Spurious: backgrounds”. Similar issues also occur in its neighborhood slices via *Attribution Mosaic*, and *AttributionScanner* automatically propagates them with higher Spuriousness.

• **What underlying factors contribute to unexpected behaviors?** ML experts are interested in understanding why such unexpected model behaviors happen. By sorting the Slice Table by descending order of *Spuriousness*, they get a list of slices with high Spuriousness possibilities. They switch *Attribution Mosaic* into the confusion matrix form (Fig. 2 E) to study further details. By clicking on the name of “*slice_35*”, they highlight this slice on the four sub-views and inspect the provided explanations, where they notice that images that lie in the “FN” group of this slice have wrong labels — they should be labeled as “not gray hair” rather than “gray hair”. They mark this issue as wrong labels and wonder whether this situation is common. By investigating its neighborhood slices on *Attribution Mosaic*, they find and mark another slice with

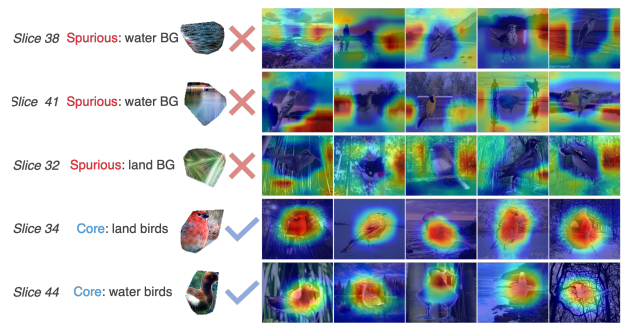


Fig. 10: Examples of findings when ML experts validate a bird category classifier, where experts identify problematic slices where the model uses backgrounds (BG) to classify birds.

wrong labels through a few clicks, *slice_2_FN*.

• **Insights summary.** Fig. 9 presents examples of the detected issues with the current model, which include wrong attributions in underperforming slices, model biases in well-performing slices, and noisy label issues. Through the aforementioned procedure in this case study, we demonstrate how *AttributionScanner* supports users to uncover and interpret potential model issues with visual summaries and other guidance. Based on annotations from ML experts, we employ the CoRM framework to mitigate the detected errors, which will be evaluated in Sec. V.

B. Bird Category Classifier Validation - Detecting Bias

• **Overview.** To study whether *AttributionScanner* can help ML experts and practitioners find the potential biases and discrimination of models, we design this case study with a biased dataset called Waterbirds [16], which is constructed by cropping out birds from images in the Caltech-UCSD Birds-200-2011 (CUB) dataset [41] and transferring them onto backgrounds from the Places dataset [42]. For each image, the label belongs to one of $\{waterbird, landbird\}$, and the image background belongs to one of $\{water\ background, land\ background\}$. The training set is skewed by placing 95% of waterbirds (landbirds) against a water (land) background and the remaining 5% against a land (water) background. Following the same data splitting as [16], the train, validation, and test sets include 4795, 1199, and 5794 images, respectively. After training and fine-tuning hyper-parameters, the waterbirds/landbirds classification model achieves 85.74% classification accuracy. In the data slice finding, we set $n_neighbors = 20$, $min_dist = 0.05$, and $n_components = 2$ for the UMAP algorithm, and $n_clusters = 46$ for K-Means.

While in this study, ML experts are aware that the model is likely biased by backgrounds — using water (land) background to classify waterbirds (landbirds). However, such priori knowledge is hard to establish in real-world applications because of the scarcity of additional well-labeled metadata. And hence the experts assume such information is unknown and want to validate whether *AttributionScanner* can make the potential model biases stand out by only utilizing the original images and the trained model.

• **Does the model exhibit bias?** To answer this key question, experts start by investigating the underperformed slices. From

TABLE II: Quantitative evaluation of the performance of the hair color classification models trained on the original and *AttributionScanner*(AS)-improved CelebA dataset.

Training Procedure	Clean Acc (↑)	Core Acc (↑)	Spurious Acc (↓)	RCS (↑)
Baseline	98.02688	97.21170	97.61917	0.067720
AS (Annotation)	98.02688	98.02185	96.92958	0.216351
AS (Propagation)	98.08225	98.16278	96.01852	0.368512

the Slice Table (Fig. 6 A), they sort slices by ascending order of accuracy and select the worst-performed *slice_38*. The coordinated information provided by *Attribution Mosaic* and model attribution heatmaps highlights a spurious correlation problem—the model uses water backgrounds to classify birds (Fig. 10). The experts annotate this slice as “spurious”, and *AttributionScanner* automatically propagates this annotation. They verify the propagation correctness on neighborhood slices and annotate *slice_41* as “spurious” with “water backgrounds” (Fig. 10). Moreover, the experts identify an underperformed *slice_32* that is not clustered with the current ones and is given a high Spuriousness possibility. They investigate it and verify that the model utilizes “Spurious feature: land backgrounds”, to predict bird classes. Through the *Attribution Mosaic* in the confusion matrix form (Fig. 6 D), they find such spurious correlations result in many false negatives (Fig. 6 DI), where the model uses land backgrounds to mistakenly predict many “waterbirds” as “landbirds”.

• **Is the detected bias prevalent across all slices? Why or why not?** ML experts are interested in determining whether the detected bias is pervasive throughout the dataset. By analyzing slices that are distant from the annotated ones in the *Attribution Mosaic* and are assigned with low Spuriousness possibilities, they discovered that the farthest neighbors, namely *slice_34* and *slice_5*, correspond to core features. This suggests that the model can correctly capture bird regions in these slices (Fig. 6 B C), which raises a follow-up “why” question. To understand in what circumstances when the model fails. They browse the original images from *slice_32* (spurious feature) and *slice_34* (core feature), respectively, as shown in Fig. 6 D and C. They find *slice_32* has very similar land backgrounds and very different birds, while on the other hand, the birds’ appearance of *slice_34* is very consistent. This finding explains why this biased model can successfully capture the core features from *slice_34* but fails at *slice_32*—greater similarities in the representation space indicate stronger features. In other words, core features in *slice_42* are strong enough to support the model’s robustness against bias. Such insights are helpful in improving model robustness and have been further studied by ML experts [43].

• **Insights summary.** A summary of insights obtained from this case study is provided in Fig. 10, where ML experts validate the existence of model biases and extract slices corresponding to different biases. In the following Sec. V, we evaluate whether *AttributionScanner* can mitigate model errors by incorporating human feedback.

V. EVALUATION

In this section, we conduct both quantitative and qualitative evaluations to validate whether *AttributionScanner* can indeed

TABLE III: Quantitative evaluation of the performance of the bird category classification models trained on the original and *AttributionScanner*(AS)-improved Waterbirds dataset.

Training Procedure	Clean Acc (↑)	Core Acc (↑)	Spurious Acc (↓)	RCS (↑)
Baseline	85.73812	82.98582	82.82901	0.004878
AS (Annotation)	89.57465	86.40534	79.81651	0.195062
AS (Propagation)	90.40867	87.40617	77.89825	0.274038

leverage human insights to enhance vision models’ performance while reducing their reliance on spurious features.

A. Quantitative Evaluation

The quantitative evaluation involves four matrices introduced in [37], including clean accuracy, core accuracy, spurious accuracy, and relative core sensitivity (RCS). We revisit their definitions as follows:

- **Clean Accuracy.** The original model accuracy, where larger values are indicative of better overall accuracy.
- **Core Accuracy $acc^{(C)}$.** The model accuracy when spurious regions are occupied with Gaussian noise, where larger values are indicative of the model’s more reliance on core regions.
- **Spurious Accuracy $acc^{(S)}$.** The model accuracy when core regions are added with Gaussian noise, where larger values are indicative of the model’s more reliance on spurious regions.
- **RCS.** This matrix quantifies the model’s reliance on core features while controlling for general noise robustness. It is defined as the ratio of the absolute gap between core and spurious accuracy, and the total possible gap for any model between core and spurious accuracy. Represented as $RCS = \frac{acc^{(C)} - acc^{(S)}}{2 \times \min(\alpha, 1 - \alpha)}$, where $\alpha = \frac{acc^{(C)} + acc^{(S)}}{2}$. RCS ranges from 0 to 1, a higher value indicative of better model performance.

In the two case studies discussed in Sec. IV, ML experts annotated five spurious slices in the CelebA dataset, $\{slice_{25}, slice_{14}, slice_{2}, slice_{44}, slice_{26}\}$, and six spurious slices in the Waterbirds dataset, $\{slice_{38}, slice_{41}, slice_{32}, slice_{29}, slice_{4}, slice_{10}\}$, respectively. For each case study, *AttributionScanner* automatically ran the Label Propagation algorithm and exported both the users’ annotation records and the propagated Spuriousness for further investigation.

To thoroughly evaluate our introduced method, we validate three models for each case. The models marked as “baseline” are the original trained models obtained at the beginning of each case study. The models marked as “*AttributionScanner*” are re-trained using the CoRM method after adding noise to “spurious” slices according to results exported from *AttributionScanner*. In particular, “Annotation” indicates that only user-annotated spurious slices were corrupted with noise, while “Propagation” indicates that propagated Spuriousness is used to identify spurious slices to be added with noise.

Table II and Table III present the quantitative evaluation results for the two case studies, respectively. Our presented *AttributionScanner* can significantly improve the vision model’s overall performance with reduced spurious correlations. Furthermore, our Label Propagation largely reduces human effort by automating the annotation process, and achieves the best performance in this quantified evaluation. Overall, our results demonstrate that *AttributionScanner* is an effective approach

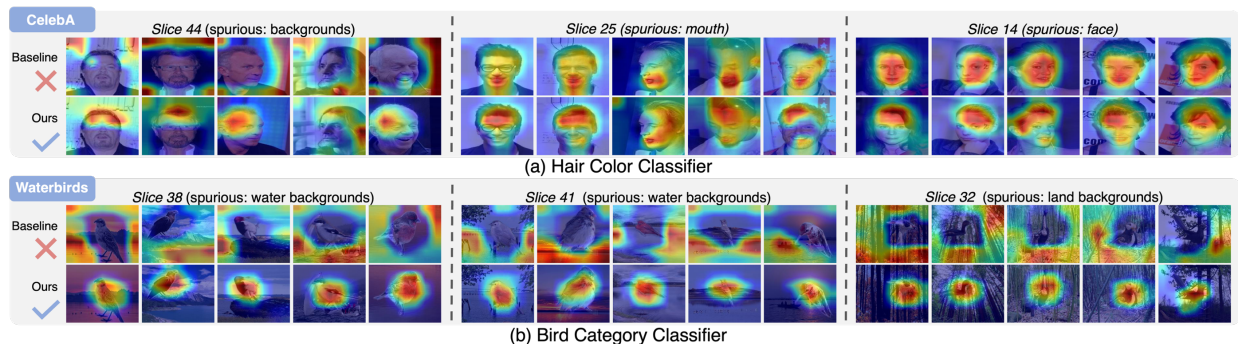


Fig. 11: Qualitative evaluation with GradCAM attribution heatmaps. We visually compare the original and the *AttributionScanner*-improved models for hair color and bird category classification, respectively. In each sub-figure, the first row refers to the original model (baseline), and the second row refers to the improved model (ours). We can observe *AttributionScanner* suppresses the spurious correlations by using the correct features for predictions.

for mitigating spurious correlations in machine learning models, and the Label Propagation algorithm is a valuable tool for automating the annotation process.

B. Qualitative Evaluation

Results in Sec. V-A highlight the best performance of *AttributionScanner* equipped with Label Propagation in mitigating spurious correlations. For further evaluation, we visually compare models’ attributions via GradCAM in Fig. 11. Refer to Sec. IV-A, the hair color classifier originally has spurious correlations dominant in $\{slice_44, slice_25, \text{and } slice_14\}$, where the model uses image backgrounds, mouth, or eyes to predict hair color, respectively. With the help of *AttributionScanner*, the model’s misattribution is successfully fixed, directing focus towards the correct hair regions (refer to Fig. 11(a)). As for the bird category classification model, it originally focuses on spurious features, water/land backgrounds, to decide whether there are water/land birds on the input image $\{slice_38, slice_41, \text{and } slice_32\}$ (refer to Sec. IV-A). In Fig. 11(b), we can observe that *AttributionScanner* mitigates these issues by helping the model to focus on the core bird features.

C. Experts Feedback

We conduct two case studies (see Sec. IV-A and Sec. IV-B) with ten ML experts to evaluate *AttributionScanner*. None of them are co-authors of this paper, and they had not previously seen *AttributionScanner*. Five are male and five are female. Six of the experts have over five years of experience in ML, two have between three to five years of experience, and two have between one to three years of experience. All experts need to conduct model validation in their research and have experience working with vision models. Our findings are drawn from their comments during the study, as they follow the “think-aloud” protocol, and additional feedback is gathered through exit discussion and questionnaire.

Summary of Likert-Type Questions. The exit questionnaire included nine Likert-type questions on a seven-point scale, aiming to evaluate *AttributionScanner* from various aspects. The feedback, as shown in Fig. 12, reflects a positive overall impression. Notably, in the usability evaluation, five

experts strongly agreed and three agreed that our system is user-friendly and understandable. In terms of effectiveness, eight experts strongly agreed that our system aids in validating models. All experts expressed strong confidence in the insights provided. Considering that Feature Inversion (FI) results are synthesized images that might initially be hard to grasp, we included questions to assess this design aspect. Seven experts strongly agreed, and two agreed that FI is helpful for understanding slice patterns. While two experts expressed neutral or somewhat disagreeing opinions about understanding slice contents based solely on FI, eight strongly agreed that *AttributionScanner*’s coordination of FI and other views supports a comprehensive understanding of slice contents. Lastly, all experts expressed interest in using our system in the future and would recommend it as a valuable tool for model validation.

Interpretable Model Validation. All experts acknowledged that *AttributionScanner* “effectively helps ML model validation”. They remarked that the complimentary visual summaries and attribution heatmaps help them “easily understand slice issues”. “It’s often hard to figure out what’s going wrong with a model”, one expert said, “This system guides me to find where I should look and explains the issues intuitively.” Another expert noted, “The ability to browse what’s happening in different slices at once greatly helped me understand the model.” They commented that they are confident about their insights because our system “highlights slice errors and provides supportive evidence”. Three of them are eager to see what issues *AttributionScanner* could uncover for the models they are currently using.

Attribution Mosaic. All participants showed particular interest in the *Attribution Mosaic* and asked about how it was designed in the interview. Seven experts were impressed by its ability to summarize model attributions across data subgroups. Two experts noted that “it highlights model issues intuitively.” Another described it as “impressive and novel,” emphasizing that it “highlights and explains the model’s failures.” Another expert commented, “This view provides a new angle for me to identify and understand the data/model issues.” All experts quickly adapted to using Spuriousness propagation and utilized the Spuriousness matrix to speed up their annotation. Specifically, five experts found that the Spuriousness propagation

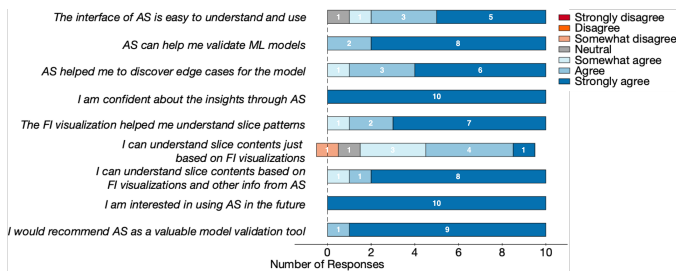


Fig. 12: Expert perception of the system, according to eight Likert-Type Questions using a 7-point scale. (AS = AttributionScanner.)

“surprisingly helpful,” and six remarked that it “really saved my effort”.

Other comments. Our experts provided feedback on additional aspects. One expert suggested that we directly display predictions and labels via text in each confusion matrix panel. “It would be better if you show ‘label: waterbirds; prediction: landbirds’ rather than ‘TN’”. Another expert discussed the potential of applying our system to validate multi-classification models. Following our brief explanation of how AttributionScanner produces results based on the model’s predicted class without restrictions on the number of classes, the expert commented, “Your system seems to be fully adaptable. And I would love to see this implementation in future work.”

VI. DISCUSSION AND FUTURE WORK

Potential risks introduced by XAI techniques. In this work, we leverage state-of-the-art XAI techniques including GradCAM and Feature Inversion, where the first is one of the most widely-adopted attribution-based explanations for neural networks [5], [44]–[46] and the second is an advanced technique to visualize what a model is looking for [33], [47], [48]. However, there has been continuing discussion on the reliability and trustworthiness of XAI techniques [26], [49], indicating the potential risks of using them. Even though both of them have been proven to retain a level of correctness through validations such as saliency checks [26], we are aware of such risks and involve human auditions in our workflow to alleviate them. In the future, we plan to design more trustworthy model explanations by reasoning about the causality relationships in model decisions [50], [51], and continue to involve human-in-the-loop to mitigate pitfalls in AI-automated tools.

Propagation approaches for the hypothetical spuriousness. We adopt the Label Propagation method [39] to automatically spread the slices’ spurious annotations from users to other slices as discussed in Sec. III-E. This is under the assumption that the distance between the slices corresponding to spurious correlations (e.g., water backgrounds) and the slices corresponding to core correlations (e.g., birds) is large. However, such assumptions can be invalid in other scenarios. For example, an image classification model trained on ImageNet [52] includes various different classes such as “husky dog” and “king penguin”. It is likely that two slices far away from each other are both corresponding to the core correlations. To address this, we plan to incorporate class similarities to

the Label Propagation matrix to improve the precision of the generated hypothetical Spuriousness.

Better guidance in data slice finding. We include the model’s performance indicators such as the classification accuracy and the average prediction confidence, as well as the Spuriousness probabilities in the Slice Table of our system to guide users to find interesting slices (refer to Fig. 2 B). Although the current guidance is proven to be effective in assisting users to detect slice issues, we plan to make further improvements. We aim to introduce new metrics calculated based on the model’s performance, the slice pattern similarity, and the Spuriousness. By doing this, we will provide more informed guidance to our users by leveraging human and model’s knowledge simultaneously, further improving the effectiveness of our model validation workflow.

VII. CONCLUSION

In this work, we present AttributionScanner, a novel human-in-the-loop model validation system empowered by metadata-free data slice finding and XAI techniques, which can support effective detection, explanation, and mitigation of potential errors and biases in vision models. To achieve this, we first present a metadata-free data slice finding method by using attribution-weighted feature vectors to group unstructured image data into data slices with consistent model attributions. Also, we design a slice pattern summarization view, Attribution Mosaic, which visually presents the shared significant patterns of each slice attributing to the model’s decision. This way, AttributionScanner is able to provide explainable data slices that reveal critical model problems, such as spurious correlations and mislabeled data. We also demonstrate the effectiveness of this work in performance improvement and bias mitigation through both quantitative and qualitative evaluations. To sum up, without additional meta-information, multi-modal model, or other background information, AttributionScanner enables an effective model validation and error mitigation workflow to alleviate underlying issues in ML models. We hope this work can inspire future research in human-AI teaming to improve AI trustworthiness and accountability.

REFERENCES

- [1] E. Pastor, L. de Alfaro, and E. Baralis, “Looking for trouble: Analyzing classifier behavior via pattern divergence,” in *Proceedings of the 2021 International Conference on Management of Data*, 2021, pp. 1400–1412.
- [2] X. Zhang, J. P. Ono, H. Song, L. Gou, K.-L. Ma, and L. Ren, “Sliceteller: A data slice-driven approach for machine learning model validation,” *IEEE Transactions on Visualization and Computer Graphics*, vol. 29, no. 1, pp. 842–852, 2022.
- [3] S. Eyuboglu, M. Varma, K. K. Saab, J.-B. Delbrouck, C. Lee-Messer, J. Dunnmon, J. Zou, and C. Re, “Domino: Discovering systematic errors with cross-modal embeddings,” in *International Conference on Learning Representations*, 2022.
- [4] D. Gunning, “Explainable artificial intelligence (xai),” *Defense advanced research projects agency (DARPA), nd Web*, vol. 2, no. 2, p. 1, 2017.
- [5] L. Rieger, C. Singh, W. Murdoch, and B. Yu, “Interpretations are useful: penalizing explanations to align neural networks with prior knowledge,” in *International conference on machine learning*. PMLR, 2020, pp. 8116–8126.
- [6] Y. Chung, T. Kraska, N. Polyzotis, K. H. Tae, and S. E. Whang, “Slice finder: Automated data slicing for model validation,” in *2019 IEEE 35th International Conference on Data Engineering (ICDE)*. IEEE, 2019, pp. 1550–1553.

- [7] S. Sagadeeva and M. Boehm, "Sliceline: Fast, linear-algebra-based slice finding for ml model debugging," in *Proceedings of the 2021 International Conference on Management of Data*, 2021, pp. 2290–2299.
- [8] E. Pastor, A. Gavgavian, E. Baralis, and L. de Alfaro, "How divergent is your data?" *Proceedings of the VLDB Endowment*, vol. 14, no. 12, pp. 2835–2838, 2021.
- [9] N. Sohoni, J. Dunnmon, G. Angus, A. Gu, and C. Ré, "No subclass left behind: Fine-grained robustness in coarse-grained classification problems," *Advances in Neural Information Processing Systems*, vol. 33, pp. 19 339–19 352, 2020.
- [10] G. d'Eon, J. d'Eon, J. R. Wright, and K. Leyton-Brown, "The spotlight: A general method for discovering systematic errors in deep learning models," in *2022 ACM Conference on Fairness, Accountability, and Transparency*, 2022, pp. 1962–1981.
- [11] B. Zhou, A. Khosla, A. Lapedriza, A. Oliva, and A. Torralba, "Learning deep features for discriminative localization," in *Proceedings of the IEEE conference on computer vision and pattern recognition*, 2016, pp. 2921–2929.
- [12] R. R. Selvaraju, M. Cogswell, A. Das, R. Vedantam, D. Parikh, and D. Batra, "Grad-cam: Visual explanations from deep networks via gradient-based localization," in *Proceedings of the IEEE international conference on computer vision*, 2017, pp. 618–626.
- [13] C. Olah, A. Mordvintsev, and L. Schubert, "Feature visualization," *Distill*, 2017, <https://distill.pub/2017/feature-visualization>.
- [14] V. Petsiuk, A. Das, and K. Saenko, "Rise: Randomized input sampling for explanation of black-box models," *arXiv preprint arXiv:1806.07421*, 2018.
- [15] G. Barash, E. Farchi, I. Jayaraman, O. Raz, R. Tzoref-Brill, and M. Zalmanovici, "Bridging the gap between ML solutions and their business requirements using feature interactions," in *Proceedings of the 2019 27th ACM Joint Meeting on European Software Engineering Conference and Symposium on the Foundations of Software Engineering*, 2019, pp. 1048–1058.
- [16] S. Sagawa, P. W. Koh, T. B. Hashimoto, and P. Liang, "Distributionally robust neural networks for group shifts: On the importance of regularization for worst-case generalization," *arXiv preprint arXiv:1911.08731*, 2019.
- [17] A. Krishnakumar, V. Prabhu, S. Sudhakar, and J. Hoffman, "Udis: Unsupervised discovery of bias in deep visual recognition models," in *British Machine Vision Conference (BMVC)*, vol. 1, no. 2, 2021, p. 3.
- [18] S. Lee, Z. J. Wang, J. Hoffman, and D. H. P. Chau, "Viscuit: Visual auditor for bias in cnn image classifier," in *Proceedings of the IEEE/CVF Conference on Computer Vision and Pattern Recognition*, 2022, pp. 21 475–21 483.
- [19] M. Kahng, D. Fang, and D. H. Chau, "Visual exploration of machine learning results using data cube analysis," in *Proceedings of the Workshop on Human-In-the-Loop Data Analytics*, 2016, pp. 1–6.
- [20] Á. A. Cabrera, W. Epperson, F. Hohman, M. Kahng, J. Morgenstern, and D. H. Chau, "FairVis: Visual analytics for discovering intersectional bias in machine learning," in *Proceedings of 2019 IEEE Conference on Visual Analytics Science and Technology (VAST)*. IEEE, 2019, pp. 46–56.
- [21] T. Wu, M. T. Ribeiro, J. Heer, and D. Weld, "Errudite: Scalable, reproducible, and testable error analysis," in *Proceedings of the 57th Annual Meeting of the Association for Computational Linguistics*, 2019.
- [22] D. Erhan, Y. Bengio, A. Courville, and P. Vincent, "Visualizing higher-layer features of a deep network," *University of Montreal*, vol. 1341, no. 3, p. 1, 2009.
- [23] A. Mahendran and A. Vedaldi, "Understanding deep image representations by inverting them," in *Proceedings of the IEEE conference on computer vision and pattern recognition*, 2015, pp. 5188–5196.
- [24] K. Simonyan and A. Zisserman, "Very deep convolutional networks for large-scale image recognition," *arXiv preprint arXiv:1409.1556*, 2014.
- [25] K. He, X. Zhang, S. Ren, and J. Sun, "Deep residual learning for image recognition," in *Proceedings of the IEEE conference on computer vision and pattern recognition*, 2016, pp. 770–778.
- [26] J. Adebayo, J. Gilmer, M. Muelly, I. Goodfellow, M. Hardt, and B. Kim, "Sanity checks for saliency maps," *Advances in neural information processing systems*, vol. 31, 2018.
- [27] C. Mao, K. Xia, J. Wang, H. Wang, J. Yang, E. Bareinboim, and C. Vondrick, "Causal transportability for visual recognition," in *Proceedings of the IEEE/CVF Conference on Computer Vision and Pattern Recognition*, 2022, pp. 7521–7531.
- [28] J. Zhuang, J. Cai, R. Wang, J. Zhang, and W. Zheng, "Care: Class attention to regions of lesion for classification on imbalanced data," in *International Conference on Medical Imaging with Deep Learning*. PMLR, 2019, pp. 588–597.
- [29] Y. Yang, B. Nushi, H. Palangi, and B. Mirzasoleiman, "Mitigating spurious correlations in multi-modal models during fine-tuning," *arXiv preprint arXiv:2304.03916*, 2023.
- [30] S. Wu, M. Yuksekogonul, L. Zhang, and J. Zou, "Discover and cure: Concept-aware mitigation of spurious correlation," *arXiv preprint arXiv:2305.00650*, 2023.
- [31] S. Lee, A. Payani, and D. H. P. Chau, "Towards mitigating spurious correlations in image classifiers with simple yes-no feedback."
- [32] L. McInnes, J. Healy, and J. Melville, "Umap: Uniform manifold approximation and projection for dimension reduction," *arXiv preprint arXiv:1802.03426*, 2018.
- [33] S. Carter, Z. Armstrong, L. Schubert, I. Johnson, and C. Olah, "Activation atlas," *Distill*, 2019, <https://distill.pub/2019/activation-atlas>.
- [34] A. Nguyen, J. Yosinski, and J. Clune, "Multifaceted feature visualization: Uncovering the different types of features learned by each neuron in deep neural networks," in *Proceedings of the International Conference on Machine Learning (ICML)*, 2016.
- [35] T. Fel, T. Boissin, V. Boutin, A. Picard, P. Novello, J. Colin, D. Linsley, T. Rousseau, R. Cadène, and T. S. Laurent Gardes, "Unlocking feature visualization for deeper networks with magnitude constrained optimization," *Advances in Neural Information Processing Systems (NeurIPS)*, 2023.
- [36] C. B. Barber, D. P. Dobkin, and H. Huhdanpaa, "The quickhull algorithm for convex hulls," *ACM Transactions on Mathematical Software (TOMS)*, vol. 22, no. 4, pp. 469–483, 1996.
- [37] S. Singla, M. Moayeri, and S. Feizi, "Core risk minimization using salient imagenet." *arXiv*, 2022.
- [38] M. A. Madaio, L. Stark, J. Wortman Vaughan, and H. Wallach, "Co-designing checklists to understand organizational challenges and opportunities around fairness in ai," in *Proceedings of the 2020 CHI Conference on Human Factors in Computing Systems*, 2020, pp. 1–14.
- [39] D. Zhou, O. Bousquet, T. Lal, J. Weston, and B. Schölkopf, "Learning with local and global consistency," *Advances in neural information processing systems*, vol. 16, 2003.
- [40] Z. Liu, P. Luo, X. Wang, and X. Tang, "Deep learning face attributes in the wild," in *Proceedings of International Conference on Computer Vision (ICCV)*, December 2015.
- [41] C. Wah, S. Branson, P. Welinder, P. Perona, and S. Belongie, "The caltech-ucsd birds-200-2011 dataset," 2011.
- [42] B. Zhou, A. Lapedriza, A. Khosla, A. Oliva, and A. Torralba, "Places: A 10 million image database for scene recognition," *IEEE transactions on pattern analysis and machine intelligence*, vol. 40, no. 6, pp. 1452–1464, 2017.
- [43] M. Zhang, N. S. Sohoni, H. R. Zhang, C. Finn, and C. Ré, "Correct-n-contrast: A contrastive approach for improving robustness to spurious correlations," *arXiv preprint arXiv:2203.01517*, 2022.
- [44] A. B. Arrieta, N. Díaz-Rodríguez, J. Del Ser, A. Bennetot, S. Tabik, A. Barbado, S. García, S. Gil-López, D. Molina, R. Benjamins *et al.*, "Explainable artificial intelligence (xai): Concepts, taxonomies, opportunities and challenges toward responsible ai," *Information fusion*, vol. 58, pp. 82–115, 2020.
- [45] P. Linardatos, V. Papastefanopoulos, and S. Kotsiantis, "Explainable ai: A review of machine learning interpretability methods," *Entropy*, vol. 23, no. 1, p. 18, 2020.
- [46] T. Ozturk, M. Talo, E. A. Yildirim, U. B. Baloglu, O. Yildirim, and U. R. Acharya, "Automated detection of covid-19 cases using deep neural networks with x-ray images," *Computers in biology and medicine*, vol. 121, p. 103792, 2020.
- [47] F. Hohman, H. Park, C. Robinson, and D. H. P. Chau, "Summit: Scaling deep learning interpretability by visualizing activation and attribution summarizations," *IEEE transactions on visualization and computer graphics*, vol. 26, no. 1, pp. 1096–1106, 2019.
- [48] E. Tjoa and C. Guan, "A survey on explainable artificial intelligence (xai): Toward medical xai," *IEEE transactions on neural networks and learning systems*, vol. 32, no. 11, pp. 4793–4813, 2020.
- [49] A. Ghorbani, A. Abid, and J. Zou, "Interpretation of neural networks is fragile," in *Proceedings of the AAAI conference on artificial intelligence*, vol. 33, no. 01, 2019, pp. 3681–3688.
- [50] J. Pearl, *Causality*. Cambridge university press, 2009.
- [51] J. Y. Halpern and J. Pearl, "Causes and explanations: A structural-model approach. part i: Causes," *The British journal for the philosophy of science*, 2020.
- [52] J. Deng, W. Dong, R. Socher, L.-J. Li, K. Li, and L. Fei-Fei, "Imagenet: A large-scale hierarchical image database," in *2009 IEEE conference on computer vision and pattern recognition*. Ieee, 2009, pp. 248–255.